Scientific Papers. Series E. Land Reclamation, Earth Observation & Surveying, Environmental Engineering. Vol. XII, 2023
Print ISSN 2285-6064, CD-ROM ISSN 2285-6072, Online ISSN 2393-5138, ISSN-L 2285-6064

EXTREME AGROCLIMATIC INDICATORS PROJECTION UNDER CLIMATE CHANGE IN OLTENIA PLANE

Denis MIHAILESCU[1, 2], Mihaela CAIAN[1], Sorin Mihai CIMPEANU[2]

[1]National Meteorological Administration, 97 Bucharest-Ploiesti Street, District 1, Bucharest, Romania
[2]University of Agronomic Sciences and Veterinary Medicine of Bucharest, 59 Marasti Blvd, District 1, Bucharest, Romania

Corresponding author email: denis.mihailescu@meteoromania.ro

Abstract

The warming of the climate system is a reality, with observations indicating increases in global average water and ocean temperatures, extensive melting of snow and ice, and global average sea level rise. It is highly likely that much of the warming can be attributed to human-caused greenhouse gas (GHG) emissions. Over the past 150 years, the average global surface temperature has risen by almost 0.8ºC overall and by 1ºC in Europe. The average global temperature in 2020 was almost identical with 2016, considered the warmest year on record. Continuing the planet's long-term warming trend, the 2020 annual average temperature was 1.02ºC higher than 1951-1980 reference average, according to NASA. 2020 slightly exceeded 2016 values, which were within the error boundaries of the analysis, making the two years the warmest on record in modern history. Here we analyse projected changes over one of the most important agricultural areas for Romania with focus on extreme agroclimatic indicators analysis.

Key words*: climate change, C3S, extreme agroclimatic indicators, climate projection.*

INTRODUCTION

Climate change is a significant change in long-term average weather conditions, so a region can become warmer, wetter or drier over several decades. A trend of change lasting a large number of years makes the difference between climate change and weather variability in its natural dynamics. Throughout its existence, the Earth has gone through periods of warming and cooling, driven by solar intensity, volcanic eruptions, and natural changes in greenhouse gas concentrations. These climate changes are considered natural. However, records show that climate change is occurring much more rapidly than in the past, especially since the mid-20th century, and cannot be explained as having natural causes alone (Turrentine et al., 2021). According to Riebeek, 2010 "These natural causes are still active today, but their influence is too small or too slow to explain the rapid warming observed in recent decades." The anthropogenic causes of climate change or more specifically the greenhouse gas emissions (GHG) they generate are the main cause of climate change at global level. Normally, greenhouse gases play an important and beneficial role in keeping the planet warm enough to be habitable. However, in recent decades, the amount of these gases in the Earth's atmosphere has increased greatly. The Intergovernmental Panel on Climate Change (IPCC, 2021) claims that concentrations of carbon dioxide, methane and nitrogen oxides are not seen in the last 800,000 years. The main contributor to climate change, carbon dioxide in the atmosphere, has increased by 40% since the beginning of the pre-industrial era. The burning of fossil fuels (oil, coal, gas) and transport represent the main source of anthropogenic emissions. Another important source is deforestation, which can come in various forms: logging, clear-cutting, fires and other forms of forest degradation. As a result, carbon is released into the air, with an estimated contribution of 20% of the total global carbon emissions. Other human activities that generate pollution are: the use of fertilizers based on nitrogen oxides, animal farms that leave behind massive emissions of methane and certain industrial activities that release fluorinated gases. And other activities that affect the land cover (agriculture, construction) can change the reflectivity of the

land surface, leading to warming or cooling (Turrentine et al., 2021). Even though forests and oceans absorb greenhouse gases from the atmosphere through photosynthesis and other processes, they cannot keep up with increasing human emissions. As a result of rapid climate change, the global temperature is increasing by about 1.18ºC since the late 19th century, with most of the warming occurring in the last 40 years. In Figure 1 is highlighted the evolution of carbon dioxide and temperature anomaly in the last 1000 years.

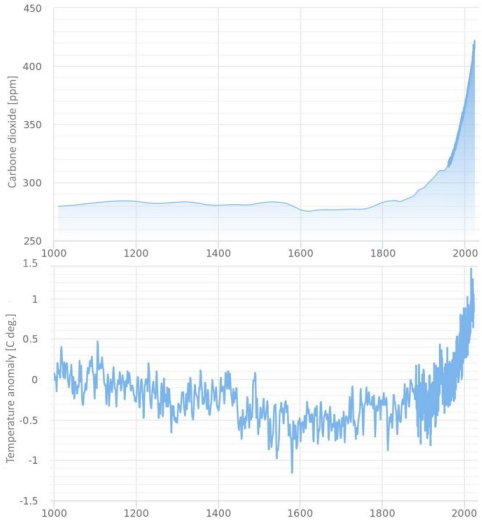

Figure 1. Carbone dioxide and temperature anomaly evolution in the last 1000 years
(source: 2degreeinstitute)

MATERIALS AND METHODS

Copernicus is the Earth observation program managed by the European Commission (copernicus.eu). It provides information acquired from satellites and in-situ data. The program is implemented
in partnership with the Member States, European Space Agency (ESA), European Organization for the Exploitation of Meteorological Satellites (EUMETSAT), European Center for Long-Range Meteorological Forecasts (ECMWF), Mercator Océan and other agencies of the European Union. All data and measurements from sensors installed on satellites, planes, ships, help service providers, public authorities and other international organizations, to make decisions to improve the quality of life at European and global level. All information made available by Copernicus services is free, open and accessible to users. The Copernicus program consists of six services, which have become operational in stages since 2012. The service, which aims at climate change, started operating in July 2018 and supports society by making available authoritative information about the past, present and future of the climate in Europe but also globally. Copernicus Climate Change Service (C3S) is based on research carried out by the World Climate Research Programme (WCRP) and responds to user requirements defined by the Global Climate Observing System (GCOS) and is an important resource for the Global Framework for Climate Services (GFCS). C3S is implemented by the European Centre for Long-Range Weather Forecasts (ECMWF) on behalf of the European Commission. The service provides data and information on the impact of climate change, for a wide range of topics and sectors of activity (water resource management, agriculture, energy, infrastructure and transport, disaster reduction, health, biodiversity, etc.), through the climate database (Copernicus Climate Data Store. C3S complements the weather and environmental services that every European country already has in place.

Climate projections are simulations of the Earth's climate in the coming decades, usually until the year 2100. They are based on possible scenarios of the evolution of concentrations of greenhouse gases, aerosols and other constituents of the atmosphere that affect the radiative balance of the planet (Climate Change Service). Climate projections are obtained by running mathematical models that can cover the entire globe or just regions. These models are known as Global Climate Models (GCM) or General Circulation Models, respectively Regional Climate Models (RCM). Most climate projections made by GCMs were part of the Coupled Model Intercomparison Project, phase 5 (CMIP5). The simulations and projections by RCM followed protocols established by the Coordinated Regional Climate Downscaling Experiment (CORDEX). C3S through CDS provides access to an important part of climate projections run under CMIP5 and CORDEX for the European domain. Climate models are

one of the main means for scientists to understand how the climate has changed in the past and might change in the future. These models simulate in detail the physics, chemistry and biology of the atmosphere, land and oceans and require some of the world's largest supercomputers to generate the climate projections (CarbonBrief, 2023). These models are continuously updated by increasing the spatial resolution, mainly, but also by adding new physical and biogeochemical processes. To make climate projections for the future, climate forcing is set to change in accordance with possible future scenarios. Scenarios represent possibilities for population growth and how quickly it will happen, how land will be used, how economies and atmospheric conditions will evolve. Before the year 1750, the Earth's average radiative forcing (net incoming minus outgoing radiation at the top of the atmosphere, [W/m^2]) was relatively constant. Human-made changes after this period in land use and greenhouse gas emissions led to an increase of radiative forcing, from 0 Wm^{-2} in 1750 to 3.18 W/m^{-2} in 2020, according to NOAA. Climatologists have defined four possible scenarios of radiative forcing (2.6, 4.5, 6.0, 8.5 W/m^2 in year 2100) that are used as input in calculating future climate. Each scenario is based on a plausible future that takes into account global greenhouse gas emissions. The scenarios, known as Representative Concentration Pathways (RCP), specify an amount of radiative forcing for the year 2100 relative to the year 1750. Unlike weather forecasts, which describe a detailed picture of conditions for the next few hours or days from now, climate models are probabilistic, indicating areas that are more likely to be warmer or colder and wetter or drier than usually. Climate models are based on global ocean and atmosphere physics and records of weather patterns that have occurred in similar ways in the past (NOAA-Climate).

Regarding actual data, **ERA-interim from ECMWF** it was initiated in 2006 to create a link between the data originally reanalysed in the ERA-40 project (1957-2002) and the next extended generation of reanalysis envisaged by ECMWF. The main objective was to improve aspects related to the representation of the hydrological cycle, the quality of the stratospheric circulation, and the management of bias and changes in the observing system. These goals were achieved largely as a result of a combination of factors, including the improvement of several parameterizations, the use of 4D variation analyses, the revised moisture analysis, the use of a variational bias correction for satellite data, and other improvements in data handling (Berrisford et al., 2011). **ERA5** is the successor to the ERA-Interim reanalysis as of 31 August 2019. It provides hourly estimates for a large number of atmospheric, oceanic and terrestrial climate variables. The data cover a global grid of 30 km and 137 atmospheric levels, from the surface to 80 km altitude. Compared to ERA-Interim, the ERA5 analysis comes with a high spatial and temporal resolution, information on quality variation in time and space, a better global balance for precipitation and evapotranspiration, an improvement in soil moisture, etc.

Climate models used in this study are from state-of the art ensemble models in CMIP5 Project that were specifically developed to overcome biases in the previous CMIP3 experiments, and are briefly described in the following (GFDL, HadGEM, MIROC, IPS, NorESM).

To better understand how Earth's biogeochemical cycles, including human actions, interact with climate, the Geophysical Fluid Dynamics Laboratory (**GFDL**) built the first NOAA-Earth System Models (**ESM**) (Dunne et al, 2012). The ESM2.1 prototype model evolved directly from the CM2.1 climate model (Delwort et al., 2006), which in turn spawned two new models representing ocean physics with alternative numerical frameworks to explore the implications of fundamental assumptions (**ESM2M** and ESM2G). The differences between the two are generally made in the physics component of the ocean. In ESM2M pressure-based vertical coordinates are used along the GFDL modular ocean model version 4.1 development path. GFDL performed all integrations with ESM2M and ESM2G for the CMIP5 protocol (Taylor et al., 2012). **HadGEM-ES** from Met Office is part of the second generation of climate models configured by the Hadley Center Global Environment Model, with new features

including a more accurate stratosphere and land system components. The individual components were successfully tuned and combined into the fully coupled model (Collins et al., 2008). The model represents interactive land and ocean carbon cycles and vegetation dynamics, with the option to prescribe either atmospheric CO_2 concentrations or anthropogenic CO_2 emissions and simulate CO_2 concentrations (Jones et al., 2011). **MIROC-ESM-CHEM** (JAMSTEC) is based on the global climate model MIROC (Model for Interdisciplinary Research on Climate), developed in partnership with the University of Tokyo, NIES and JAMSTEC. It is composed of a general atmospheric circulation model (MIROC-AGCM 2010) that includes an on-line aerosol component (SPRINTARS 5.00), an ocean model (COCO 3.4) and a land surface model (MATSIRO), all of which being coupled in MIROC (Watanabe et al., 2011). MIROC-ESM additionally comes with an atmospheric chemistry component (CHASER 4.1), an ocean nutrient-phytoplankton-zooplankton-detritus (NPZD) component, and a terrestrial ecosystem (vegetation dynamics) component (SEIB-DGVM). **IPSL-CM5A-LR** is the 5th version of the model developed by the Institut Pierre Simon Laplace (IPSL). In addition to the atmosphere-ocean-land-surface-ice components, it also includes a representation of the carbon cycle, stratospheric and tropospheric aerosol chemistry. The IPSL-CM5A-LR model incorporates an ORCHIDEE surface model into the LMDZ5A atmospheric component. It is coupled with the NEMOv3.2 ocean module which includes the LIM-2 ice model and the PISCES biogeochemistry model. The coupling between the two models (atmospheric and oceanic) is done using the OASIS3 software (Valcke, 2006). Includes 31 vertical levels with the best resolution in the first 150 m at the top (Peresechino et al., 2013). **NorESM1-M** is mostly based on CCSM4 (Community Climate System Model, version 4), but differs by using an isopycnic ocean module and replacing the CAM4 atmospheric mode with CAM4-Oslo (Bentsen et al., 2013). The CCSM4 components are coupled through CPL7 (Craig et al., 2012) which manages overall control of model execution and information exchange between components. Inside the coupling is a top-level driver that organizes the coupled model into a single executable and issues calls to the initialization, run, and completion routines for each component of the model (Bentsen et al., 2013).

Focuses of this work, the agroclimatic indicators are useful because they "translate" climate variability and changes into useful terms for the agricultural sector (Agroclimatic Indicators, 2019). They are often used in species distribution modeling to study plant phenological evolutions under varied climatic conditions. For many users in the agricultural community, crop development assessments for current or future crop seasons are particularly important. This is especially true for agricultural policy and business environments, as early indications of production anomalies are of critical importance for taxes/subsidies and price volatility. The provision of pre-processed agroclimatic indicators facilitates availability to the user and will facilitate the use of climate data by the agricultural community. Agroclimatic indicators are based on formulas that measure factors and climatic conditions that can affect vegetation positively or negatively and can correlate with the main type of vegetation of an area. They are used in agriculture to reconstruct climate and environmental changes such as: climate-induced phases in plant growth, amount of moisture and heat, drought, etc. (Agroclimatic Indicators, 2019). There are two main categories of indicators calculated directly from climate variables, which C3S makes available pre-calculated, along with the workflow for on-demand generation of specific indicators:

- Generic Agroclimatic Indicators: represent aggregations, accumulations or frequencies calculated according to a certain atmospheric variable (temperature and precipitation);
- Crop-specific indicators: require information on the date of sowing and harvesting, the growing range of minimum and maximum temperatures, etc. to produce products specific to the culture of interest.

C3S produces a total of 26 indicators with global coverage calculated from daily data, derived from two essential climate variables (ECVs):

- Surface air temperature: daily minimum air temperature at 2 m (TN), daily maximum air temperature at 2 m (TX) and daily mean air temperature at 2 m (TG);
- Precipitation: daily total (RR).

The indicators were adapted from the collection of the European Climate Assessment & Dataset (ECA & D) project, for their relevance in agriculture but not oriented towards a certain type of culture. Data description is presented in Table 1.

Table 1. Spatial and temporal characteristics (source: CDS Service)

Data type	Gridded
Projection	Regular latitude-longitude grid
Horizontal coverage	Global
Horizontal resolution	0.5° x 0.5°
Vertical coverage	Surface
Vertical resolution	Single level
Temporal coverage	1951-2099
Temporal resolution	10-day, Seasonal, Annual
File format	netCDF-4

To generate historical and future agroclimatic indicators, climate data with bias corrections made available through the ISIMIP project (Inter-Sectoral Impact Model Intercomparison Project) were used. Bias correction is a process of scaling climate model outputs to account for systematic errors in order to improve correlation with observed data (Soriano et al., 2019). ISIMIP was organized into 3 main simulation rounds, from which the ISIMIP Fast Track products formed the basis of the current set of indicators. For each simulation run a set of gridded and corrected climate variables were produced to be used as input data in running the impact models. These climate datasets contain bias correction for climate data from 5 CMIP5 models covering the period 1950-2099, daily temporal resolution and downscaling to 0.5° x 0.5° lat-lon globally. For historical observations, the WFDEI - Watch Forcing data methodology applied to ERA-Interim dataset (Weedon et al., 2014) was used to generate agroclimatic indicators from the climatological period 1981-2010. The temperature bias correction algorithm preserves GCM monthly mean values by adding a compensation constant for each grid point and month. In this way, the absolute temperature changes are not modified by the bias correction, but the reference level is adjusted to the level of observations over the period of 40 years. The minimum and maximum temperature (Tmin. and Tmax.) are also corrected for systematic bias. The algorithm ensures that for the historical period, the average distance between the maximum (or minimum) daily temperature value and the average daily temperature (T) is maintained. This is achieved by calculating a factor for the historical period:

$$K = \text{mean}\,[\text{Tmin. (max.)}_{Watch} - T_{Watch}] / \text{mean}\,[\text{Tmin. (max.)}_{GCM} - T_{GCM}] \quad (1)$$

and the corrected bias for the maximum (minimum) temperature is given by the relation:

$$\text{Tmin. (max.)}_{BC} = k\,[\text{Tmin. (max.)}_{GCM} - T_{GCM}] + T_{GCM} \quad (2)$$

The daily variability of the temperature data is adjusted to reproduce the variability of the observed data. The data is processed by:

- subtracting the monthly averages from both sets of data;
- multiplying the daily residual variations with a monthly constant and specific factor per grid point, thus correlating the variations of the simulations with observations;
- the daily variation with bias correction is subsequently added to the corrected monthly averages provided by the GCM.

For the precipitation data, a multiplicative correction was used to adjust the historical monthly mean values to the observed climatological monthly mean values. This ensures that the monthly precipitation values are kept up to a constant multiplier factor. Monthly averages are multiplied by a grid point and a constant monthly correction factor (one for each month). It therefore ensures that the relative change in precipitation, as described by the original GCM data, is preserved. In combination with the temperature correction, the hydrological sensitivity of the GCM (relative change in precipitation per degree of warming) was preserved. To adjust the daily variability of precipitation, a multiplicative method was also adopted that adjusts the relative variability. The data is processed as follows:

- normalization of daily precipitation data from GCM and observed (Watch) data by dividing by their monthly mean values. The daily variability of months without precipitation, specified by a certain threshold, is not changed;
- after normalizing wet months, the distribution of simulated data is correlated to the distribution of observed daily data using a transfer function (Piani et al., 2010). This function corrects both the frequency of dry days and the distribution of precipitation intensity to the observed statistics;
- for the projections, the transfer function is applied to the normalized daily precipitation for wet months;
- multiplying the transferred data with monthly average values with bias correction. By ensuring that the mean values of the normalized daily data transferred is equal to one (by dividing by the associated mean value), it ensures that the corrected monthly mean values are preserved when daily variability is taken into account.

For the other variables (monthly and daily) the same multiplicative approach as for precipitation was used. In the case of the monthly variables, the only exception is the wind, its magnitude being corrected using a multiplicative algorithm, its individual components being then derived by preserving the direction from the original GCM data.

From 26 indicators, 6 were selected with a temporally resolution of 10 days. Thus, each processed indicator contains 1080 time steps for each period of 30 years. Data processing was done with Climate Data Operators (CDO) and cartographic representations in ArcGIS. The historical climatological period includes the interval 1981-2010 and the projections were made for 2 periods, 2011-2040 (near future) and 2041-2070 (near-medium future). The scenarios for which simulations were made are: RCP4.5 (medium radiative forcing) and RCP8.5 (high radiative forcing). Data from all 5 models were used in assembled format from which the historical period was subtracted. The cartographic products are made for the fields over Romania and represent time averages (30 years) of each indicator for the 2011-2040 (P1) and 2041-2070 (P2) projections. The graphic products are made strictly on the Oltenia Plain and represent the estimates of expected long-term variability under climate change. The location of Oltenia Plain, in the south-western Romania, the overlapping of the Danube terraces, the sandy soils and other topoclimatic features, make drought and associated phenomena occur annually in this area. The multi-model ensemble was used in order to cover the inherent modeling uncertainty. To create the graphs, the moving average was calculated with a period of 150 time steps (one time step = 10 days), thus eliminating waves with a period of less than approximately 4 years. Finally, the data were averaged for the entire surface of the Oltenia Plain and represented.

RESULTS AND DISCUSSIONS

Heavy precipitation days (R 10 mm)

It represents the number of days in which at least 10 mm of precipitation was recorded over a period of 10 days (Figure 2). It provides useful information for possible crop damage and losses due to runoff. The trend of the R 10 mm indicator is to migrate to the north and northwest of the country, a fact that is best observed in P2. In Oltenia Plain, the change values are low, between 0-0.024 days/10 days in P1 (compared with Hist), but also in the RCP4.5 scenario in P2 (compared with Hist). Note the eastern part of the plain, which overlaps the areas where sand dunes have developed, where the R 10 mm changes are minimal in both scenarios and periods. In the first part of P2, the heavy precipitation has an increasing tendency and higher values than Hist especially in western part of Oltenia Plain, in both scenarios (mainly RCP8.5) but after 2060 they will decrease quickly to negative differences compared to Hist (making an overall negative trend of differences over the whole period) (Figure 3).

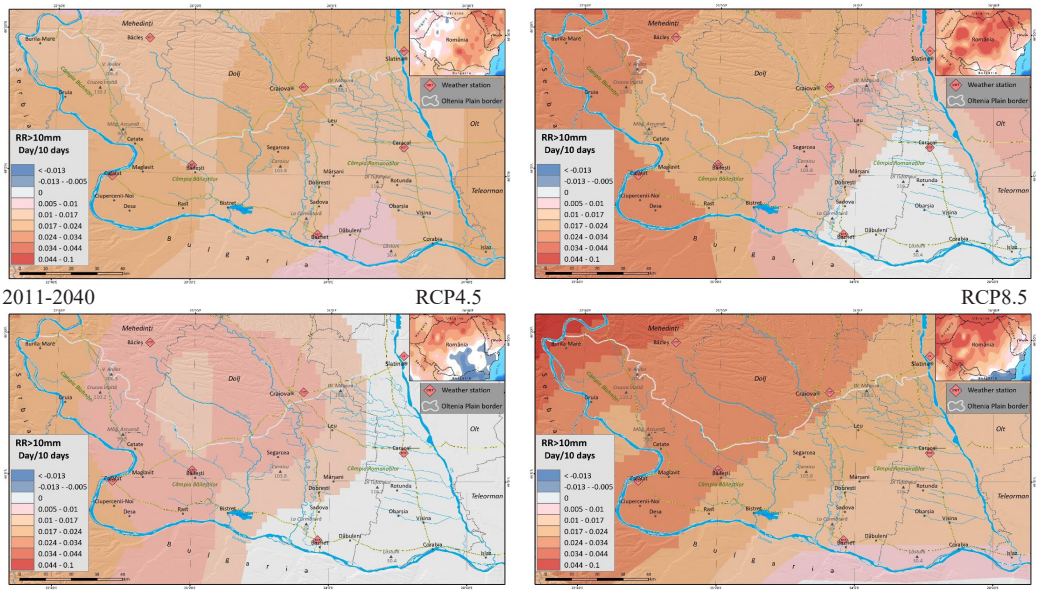

Figure 2. Heavy precipitation days projected changes in scenarios compared with Hist

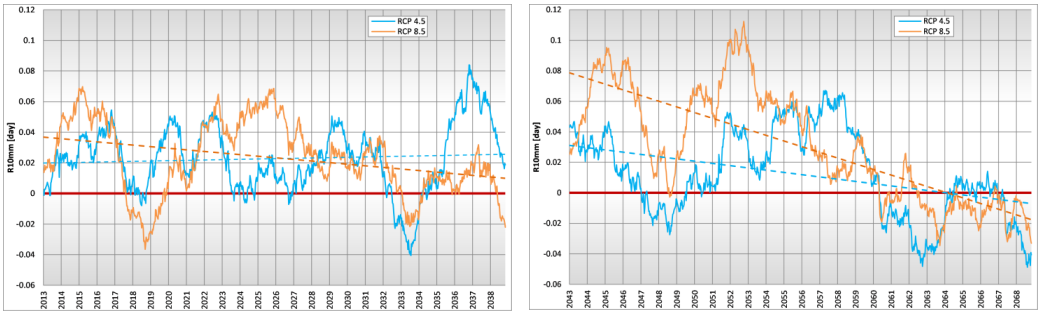

Figure 3. Heavy precipitation days trend for P1-Hist (left 2011-2040) and P2-Hist (right 2041-2070)

Very heavy precipitation days (R 20 mm)

It represents the number of days in which at least 20 mm of precipitation was recorded over a period of 10 days (Figure 4). It provides information on extreme possible crop damage and losses due to runoff. The R 20 mm indicator differences (scenarios minus Hist), follows the R 10 mm trends, with values very slightly above 0 for both scenarios until the year 2034. Quite similar to R10mm, after this year and continuing in P2, the values oscillate between 0 and 0.017 days/10 days, generally being a period of increasing values (Figure 5). Due to the global warming trend, warm air holds more water vapor in the atmosphere, which in turn can produce extreme events in the form of precipitation. Dynamical changes have also a contribution to regional changes in these extremes. Increasing R 20 mm values does not always also lead to increased accumulated precipitation, but the amounts that fall during extreme events can increase, which is already observed during the latest decades.

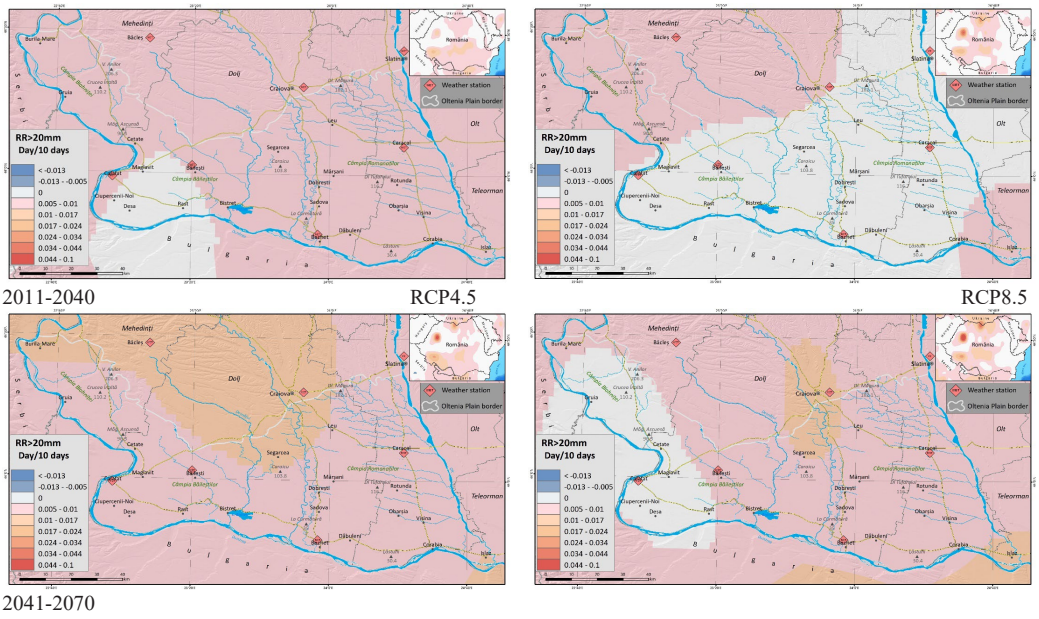

Figure 4. Very heavy precipitation days projected changes in scenarios compared with Hist

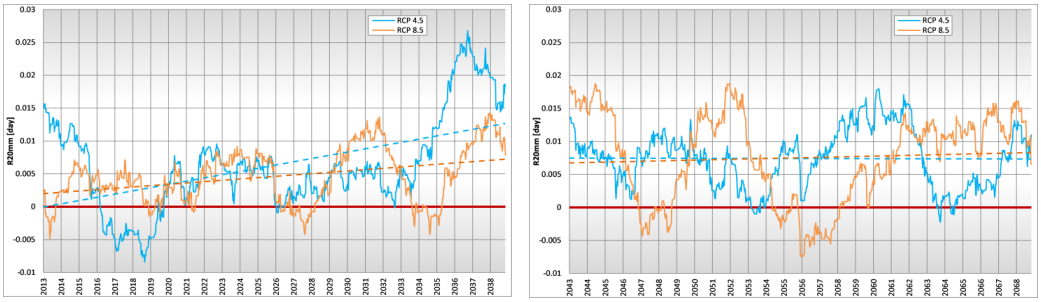

Figure 5. Very heavy precipitation days trend in P1-Hist (left 2011-2040) and P2-Hist (right 2041-2070)

Precipitation sum (RR)

RR is the sum of accumulated precipitation in 10 days. The indicator provides information about the excess or reduction of the water reserve. A wet day has RR = 1 mm while a dry day has RR<1 mm (Figure 6). In P1, both scenarios indicate positive RR differences values compared with Hist and slightly higher in RCP8.5. Towards the end of the period, the difference values (relative to Hist) become clearly negative in average for both scenarios (but however later in P2 with some still increase in P2 in the first part, more in RCP8.5). Even though extreme precipitation tends to increase, moderate precipitation is decreasing in P2, having the effect of reducing cumulative precipitation. RR drops strongly in the second half of P2, its negative values indicating periods of dryness for very long periods of time (Figure 7).

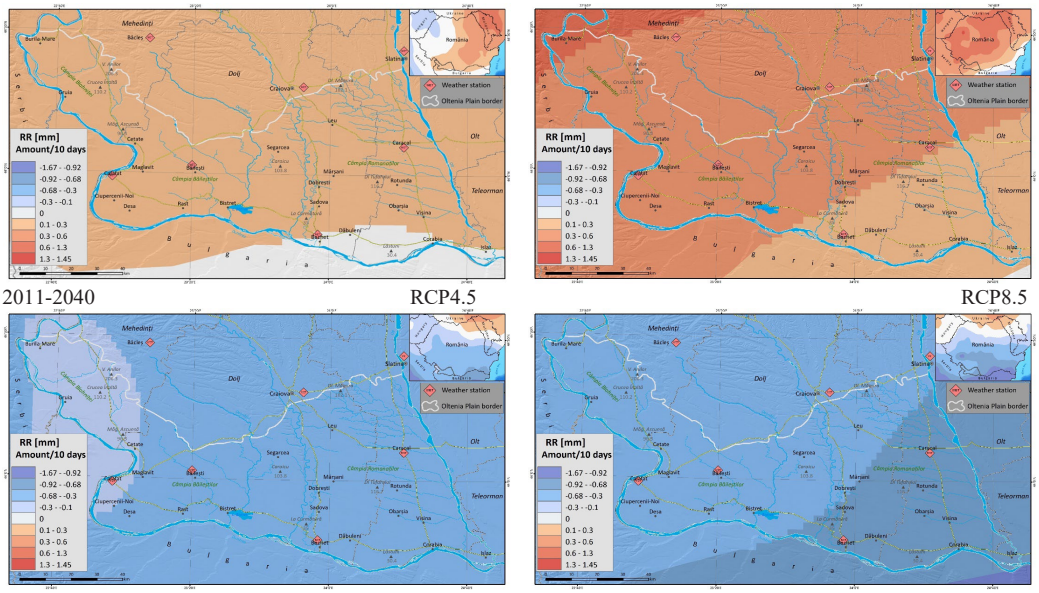

Figure 6. Precipitation sums projected changes in scenarios compared with Hist

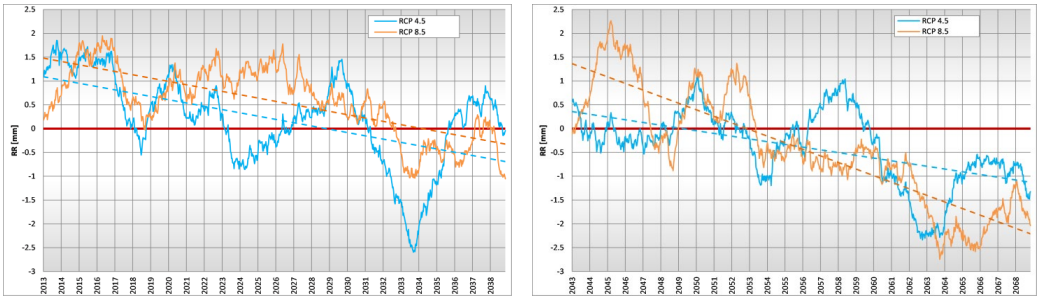

Figure 7. Precipitation sum trend in P1-Hist (left 2011-2040) and P2-Hist (right 2041-2070)

Mean of daily mean temperature (TG)

Average TG values for a 10-day interval where TG represents the average daily temperatures (Figure 8). It provides information on long-term climate variability and change. In P1, the TG values indicate an increase compared to the historical period with an average of approximately 1.2ºC in the RCP4.5 scenario and nearly 1.5ºC in the RCP8.5.

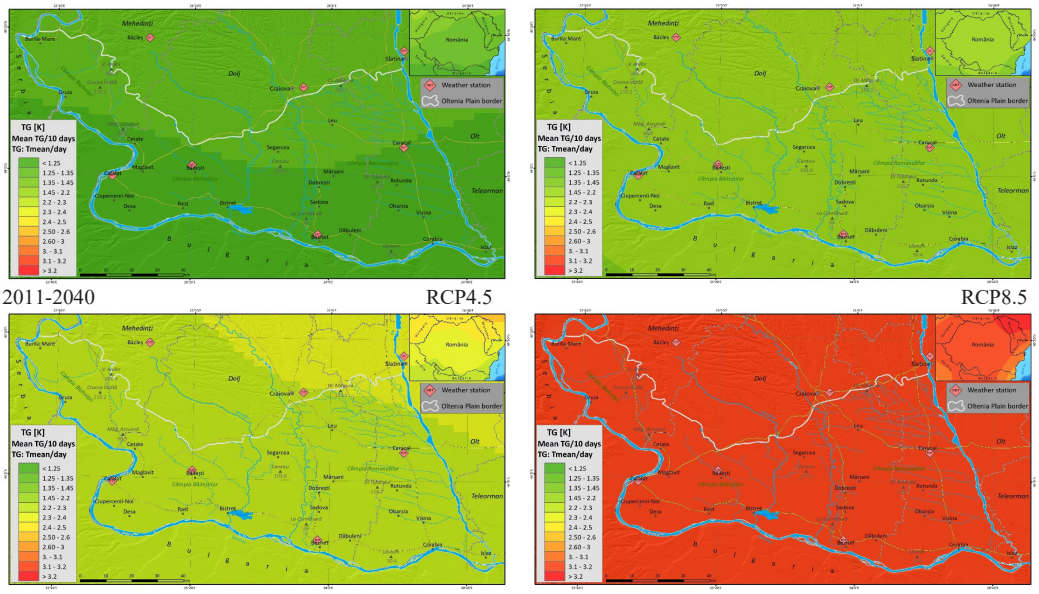

Figure 8. Mean of daily mean temperature projected changes in scenarios compared with Hist

In P2 both scenarios indicate almost double TG increases (relative to Hist) compared to P1, starting in 2050. If over 4-year period RCP4.5 stabilizes at an average value of about 2ºC, RCP8.5 forecasts a TG increase of average 3ºC, punctually even exceeding the value of 3.5ºC (after 2053) and frequently after 2060 (Figure 9).

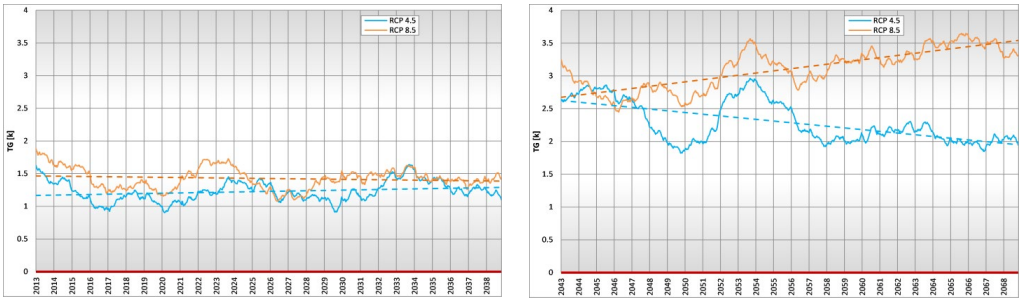

Figure 9. Mean of daily mean temperature trend in P1-Hist (left 2011-2040) and P2-Hist (right 2041-2070)

Summer days (SU)

The number of days relative to a 10-day period in which the maximum daily temperature TX >25ºC (Figure 10). It provides indications of the occurrence of heat stress and is useful for specific crop variants for heat/cold stress (above/below optimal temperature thresholds). SU fluctuates quite a lot over periods of about 10 years, an aspect that stands out in both periods. However, the general trend is to increase the number of days with temperatures higher than 25ºC compared to Hist. In P2, SU differences reaches double values compared to P1, after 2050 (Figure 11).

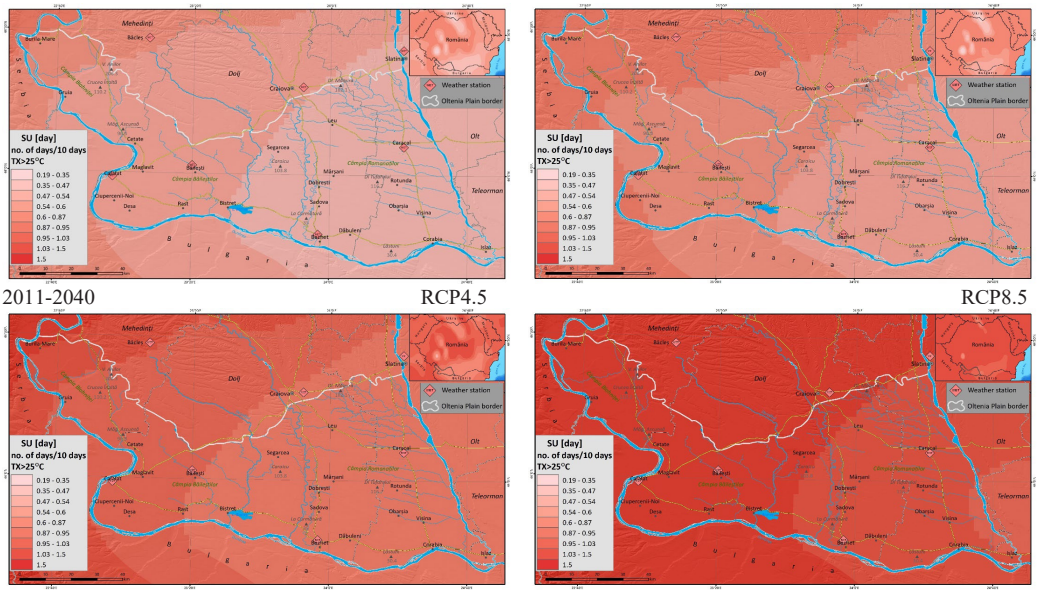

Figure 10. Summer days projected changes in scenarios compared with Hist

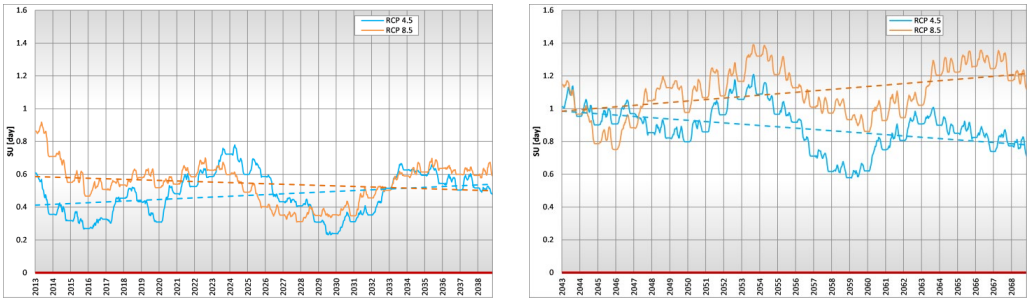

Figure 11. Summer days trend in P1-Hist (left 2011-2040) and P2-Hist (right 2041-2070)

CONCLUSIONS

The current context requires an accelerated effort at the international and national level in terms of monitoring and understanding the mechanisms of the evolution of climatic and environmental parameters in the context of climate change, in order to be able to develop methods to counter their effects in a timely manner. Unfortunately, the time scale and speed with which these events become more intense and accelerated is short, many times shorter than the time in which such mitigation measures can be developed. However, current climate scenarios project important changes both at the country and regional level. Agroclimatic indices analysed for the Oltenia Plain, very clearly forecast the increase in temperatures (averages, minimums, daily maximums) and the increase in extreme precipitation (in spite of overall RR mean decrease) that lead to the destruction of crops due to thermal stress and water runoff from precipitation. At the same time, soil fertility decreases due to surface washing. In the context where the Oltenia Plain is already affected by drought (especially agricultural) and its associated phenomena (aridization and desertification), the increase in temperatures above the thresholds of 1.5°C and 2°C can lead to catastrophic effects for specific agricultural crops. Because of this, changes can occur in the pattern of crops that can be replaced by other species resistant to heat stress, such as exotic

cultures. These projected values should be a warning and the decision-makers should get involved in the development of environmental policies that reduce the effect of climate change in Romania and in particular in the Oltenia Plain.

REFERENCES

2degree Institute. Retrieved from https://www.2degreesinstitute.org/

Agroclimatic indicators - Product User Guide and Specification (2019). C3S Global Agriculture SIS, Issued by Telespazio VEGA, UK.

Bentsen, M., Bethke, I., Debernard, J. B., Iversen, T., Kirkevåg, A., Seland, Ø., Drange, H., Roelandt, C., Seierstad, I. A., Hoose, C., and Kristjánsson, J. E. (2013). The Norwegian Earth System Model, NorESM1-M - Part 1: Description and basic evaluation of the physical climate. *Geosci. Model Dev., 6,* 687-720, doi.org/10.5194/gmd-6-687-2013

Berrisford, P., Dee, D., Poli, P., Brugge, R., Fielding. K., Fuentes, M., Kalberg, P., Kobayashi, S., Uppala, S., Simmons, A. (2011). *ERA report series, The ERA-Interim archive, Version 2.0*. ECMWF Publications, Reading, UK.

CarbonBrief. Retrieved from https://www.carbonbrief.org/

Climate Data Operators (CDO). Retrieved from https://code.mpimet.mpg.de/projects/cdo/

Collins, W.J., Bellouin, N., Doutriaux-Boucher, M., Gedney, N., Hinton, T., Jones, C.D., Liddicoat, S., Martin, G., O'Connor, F., Rae, J., Senior, C., Totterdell, I., Woodward. S. (2008). *Evaluation of the HadGEM2 model*. Met Office Hadley Centre, Exter, UK.

Copernicus. Retrieved from https://www.copernicus.eu/

Copernicus Climate Change Service. Retrieved from https://climate.copernicus.eu/

Copernicus Climate Data Store. Retrieved from https://cds.climate.copernicus.eu/

Craig, A., Vertenstein, M., Jacob, R. (2021). A new flexible coupler for earth system modeling developed for CCSM4 and CESM1. *Int. J. High Perform. Comput. Appl., 26*, 31–42, doi.org/10.1177/109434201142814

Delworth, T., Broccoli, A., Rosati, A., Ronald, S., Balaji, V., Beesley, J., Cooke, W., Dixon, K., Dunne, J., Dunne, K.A., Durachta, J., Findell, K., Ginoux, P., Gnanadesikan, A., Gordon, C., Griffies, S., Gudgel, R., Harrison, M., Held, I., Zhang, R. (2006). GFDL's CM2 Global Coupled Climate Models. Part I: Formulation and Simulation Characteristics. *Journal of Climate, 19*. 643-674. 10.1175/JCLI3629.1.

Intergovernmental Panel on Climate Change (2021). *Climate Change 2021, The physical Science Basis. Summary for policymakers*. ISBN 978-92-9169-158-6

Jones, C. D., Hughes, J. K., Bellouin, N., Hardiman, S. C., Jones, G. S., Knight, J., Liddicoat, S., O'Connor, F. M., Andres, R. J., Bell, C., Boo, K.-O., Bozzo, A., Butchart, N., Cadule, P., Corbin, K. D., Doutriaux-Boucher, M., Friedlingstein, P., Gornall, J., Gray, L., Halloran, P. R., Hurtt, G., Ingram, W. J., Lamarque, J.-F., Law, R. M., Meinshausen, M., Osprey, S., Palin, E. J., Parsons Chini, L., Raddatz, T., Sanderson, M. G., Sellar, A. A., Schurer, A., Valdes, P., Wood, N., Woodward, S., Yoshioka, M., and Zerroukat, M. (2011). The HadGEM2-ES implementation of CMIP5 centennial simulations, *Geosci. Model Dev.*, 4, 543–570, https://doi.org/10.5194/gmd-4-543-2011

National Aeronautics and Space Administration (NASA). Retrieved from https://www.nasa.gov/

Natural Resources Defense Council (NRDC). Retrieved from https://www.nrdc.org/

National Oceanic and Atmospheric Administration (NOAA). Retrieved from
https://www.noaa.gov/; noaa.gov/climate

Peresechino, A., Mignot, J., Swingedouw, D., Labetoulle, S., Guilyardi, E. (2012). Decadal predictability of the Atlantic meridional overturning circulation and climate in the IPSL-CM5A-LR model. *Clim Dyn 40*, 2359-2380, doi.org/10.1007/s00382-012-1466-1

Piani, C., Weedon, P.G., Best, M., Gomes, S., Viterbo, P., Hagemann, S., Haerter, J.O. (2010). Statistical bias correction of global simulated daily precipitation and temperature for the application of hydrological models. *J. Hydrol., 395*, 199–215.

Riebeek, H. (2010). *Global Warming*. NASA Earth Observatory. Retrieved from https://earthobservatory.nasa.gov/features/GlobalWarming

Soriano, E., Medeiro, L., Garijo, C. (2019). Selection of bias correction methods to assess the impact of climate change on flood frequency curves. MDPI *Water, 11*, 2266, doi.org/10.3390/w11112266

Taylor, K.E., Stouffer, R.J., Meehl, G.A. (2012*).* An overview of CMIP5 and experiment design. *Bull. Amer. Meteor. Soc., 93*, 485-498, https://doi.org/10.1175/BAMS-D-11-00094.1

Turrentine, J., Denchak, M. (2021). *What is climate change?* National Resources Defence Coincil. Retrieved from https://www.nrdc.org/

Valcke, S. (2006). *OASIS3 user guide (prism_2-5), technical report TR/CMGC/06/73, PRISM Report No 2*. P 60, CERFACS, Toulouse, France.

Watanabe, S., Hajima, T., Sudo, K., Nagashima, T., Takemura, T., Okajima, H., Nozawa, T., Kawase, H., Abe, M., Yokohata, T., Ise, T., Sato, H., Kato, E., Takata, K., Emori, S., and Kawamiya, M. (2011). MIROC-ESM 2010: model description and basic results of CMIP5-20c3m experiments, *Geosci. Model Dev., 4*, 845–872, https://doi.org/10.5194/gmd-4-845-2011.

Weedon, P.G., Balsamo, G., Bellouin, N., Gomes, S., Best, J.M., Viterbo, P. (2014). The WFDEI meteorological forcing data set: WATCH Forcing Data methodology applied to ERA-Interim reanalysis data. *Water Resources Research, 50*(9), doi.org/10.1002/2014WR015638